Journal of Alloys and Compounds, 197 (1993) 7–16
JALCOM 610

Development of TRAIL, a simulation code for the molten salt electrorefining of spent nuclear fuel

Tsuguyuki Kobayashi* and Moriyasu Tokiwai
Fast Breeder Reactor Division, Komae Laboratory, Central Research Institute of Electric Power Industry, 2-11-1 Iwadokita, Komae-shi, Tokyo 201 (Japan)

(Received September 4, 1992)

Abstract

A simulation code for the molten salt electrorefining of spent metallic nuclear fuel from the Integral Fast Reactor has been developed. This code (named TRAIL) employs diffusion layer theory in the vicinity of the electrodes. Model parameters such as the diffusion layer thickness were determined from polarization data measured with uranium at different concentrations in the molten salt electrolyte and liquid cadmium anode of an electrorefining cell. Calculations were made to verify the code with experimental data for various operational modes. Good agreement with the data was obtained. It was also found that this code can provide useful information to aid in understanding the electrotransport process within the electrorefiner.

1. Introduction

The application of a pyrometallurgical process to the recycling of spent metallic nuclear fuel has been developed at Argonne National Laboratory (ANL) as part of the Integral Fast Reactor (IFR) project [1]. In this process, U–Pu–Zr alloyed metallic fuel irradiated in a fast breeder reactor (FBR) is electrorefined in molten salt (LiCl–KCl eutectic) to separate the fission products (FPs) from heavy metals such as uranium and plutonium. The recovered heavy metals are then injection cast to make fuel slugs for the fabrication of new fuel assemblies.

This innovative metallic fuel cycle (MFC) has the following advantages over the conventional PUREX-based, multistage aqueous reprocessing used for oxide fuels.

(1) The process simplicity could yield an economical nuclear fuel cycle for FBRs.

(2) The use of salt as an electrolyte is more desirable for handling highly radioactive FBR spent fuels than is the use of organic solvents (such as tri-*n*-butyl phosphate), which disintegrate under heavy irradiation.

(3) The mass of fissile material to reach criticality in the salt is less restrictive compared with that in water, which is a good neutron moderator.

(4) Minor actinides such as neptunium, americium and curium are expected to accompany plutonium and thus be transmuted into stable or short-lived FPs in FBRs.

A schematic representation of a typical electrorefiner (ER) for this process is shown in Fig. 1. The ER will contain molten salt (LiCl–KCl eutectic) and liquid cadmium at 773 K in a low carbon steel vessel. The following dual-cathode operations [2, 3] will be utilized for the recovery of heavy metals from the spent metallic fuels.

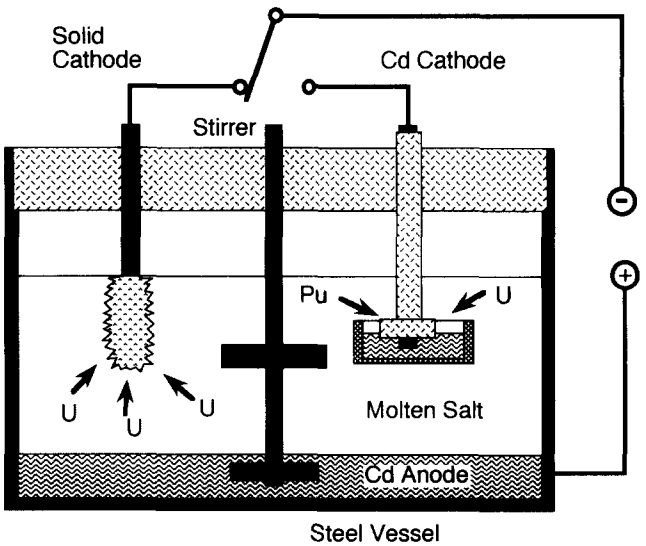

Fig. 1. Schematic set-up for electrorefining of spent metallic fuel. Uranium is first removed by the solid cathode, then plutonium is deposited with uranium on the Cd cathode.

*Present address: Advanced Reactor Engineering Department, Isogo Engineering Center, Toshiba Corp., 8, Shinsugita, Isogo, Yokohama 235, Japan.

0925-8388/93/$6.00

(1) The spent fuels are anodically dissolved in the salt. At equilibrium, alkaline, alkaline earth and lanthanide FPs tend to distribute in the salt as chlorides, while noble metal FPs are expected to stay in the cadmium as metals. Uranium and plutonium distribute in both the salt and cadmium.

(2) Only uranium is reduced from the salt and deposited on the solid cathode (low carbon steel), because uranium chloride is the easiest to reduce on the solid cathode among the heavy metal chlorides such as plutonium chloride. As a result, plutonium chloride builds up in the salt during several batch operations of the solid cathode. In many prior experiments this uranium has been deposited after the anodic dissolution. However, in the actual process the deposition will be done at the same time as the anodic dissolution to improve the throughput.

(3) When the concentration of plutonium chloride in the molten salt reaches the desired value, the solid cathode is replaced with a liquid cadmium cathode (hereafter referred to as the Cd cathode), which consists of a ceramic crucible filled with liquid cadmium. In this cathode, plutonium and other minor actinides codeposit with uranium, because their reduction potential approaches that of uranium, owing to their very low activity coefficients in cadmium.

The material transport during the above electrorefining is rather complicated. There are many kinds of FPs with different electrochemical properties and the heavy metals are collected by two types of cathode, *i.e.* the solid cathode and the Cd cathode. Therefore a computer simulation of the process would be useful not only to better understand the experimental data but also to control the operation of the electrorefiners. In Japan, CRIEPI (Central Research Institute of Electric Power Industry) has been studying the feasibility of the MFC through collaboration with the US Department of Energy (DOE) and Japanese manufacturers. This paper describes the TRAIL (*Tr*ansportation of *Act*inides in E*l*ectrorefiner) code developed at CRIEPI. The basic parameters for the code were determined by Japanese experimental data [4, 5] obtained with an electrorefiner using a simulated metallic fuel of uranium and lanthanides. The TRAIL code has been verified by data including plutonium obtained at ANL.

2. Calculation model

At the ER operation temperature of 773 K the activation and reduction processes on the anode and cathode surfaces are assumed to be so rapid that they are always in equilibrium. For example, the following Nernst equation holds at the cadmium–salt interface of the Cd anode:

$$E_a = E_o^x + \frac{RT}{Z_x F} \ln\left(\frac{\gamma_x^{salt} X_{as}^{salt}}{\gamma_x^{cd} X_{as}^{cd}}\right) \quad (1)$$

where E_a (V) is the anode potential, E_o^x (V) is the standard potential of element X, $R = 8.314$ J mol^{-1} K^{-1} is the gas constant, T (K) is the temperature, Z_x is the number of equivalents per mole of X in the salt, $F = 96\,485$ C mol^{-1} is the Faraday constant, γ_x^{salt} is the activity coefficient of X in the salt, γ_x^{cd} is the activity coefficient of X in cadmium, X_{as}^{salt} (mol cm^{-3}) is the concentration of X at the salt side of the Cd–salt interface and X_{as}^{cd} (mol cm^{-3}) is the concentration of X at the cadmium side of the Cd–salt interface.

The code assumes uniform concentrations of the elements in the salt and cadmium, except in the vicinity of the electrode interfaces. The mass transfer is modelled by diffusion layer theory, in which the concentration gradients in the vicinity of the electrode surface are approximated as linear within the thin diffusion layer. For example, the assumed concentration profile in the vicinity of the Cd anode is shown in Fig. 2. In this case the anodic current density carried by each element X can be calculated as follows:

$$i_x^a = Z_x F D_x^{cd} \frac{X_b^{cd} - X_{as}^{cd}}{\delta_a^{cd}} \quad (2a)$$

$$= Z_x F D_x^{salt} \frac{X_{as}^{salt} - X_b^{salt}}{\delta_a^{salt}} \quad (2b)$$

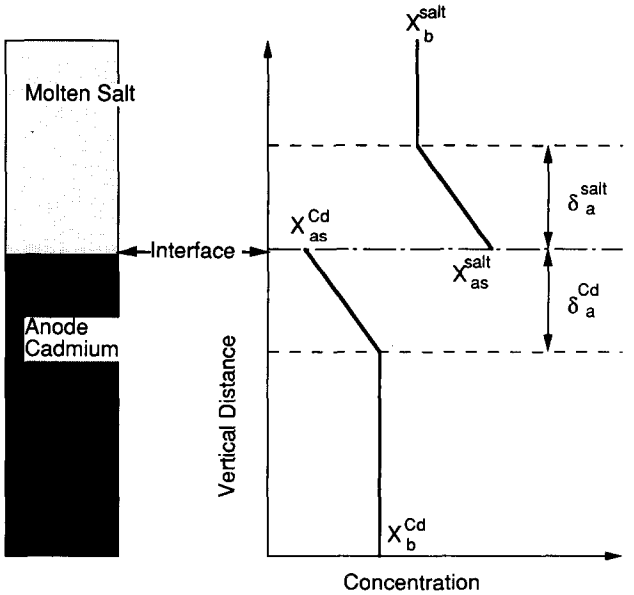

Fig. 2. Diffusion layer model for the Cd anode. The concentration gradients in the vicinity of both sides of the salt–Cd interface are approximated as linear within the thickness of the diffusion layer.

where i_x^a (A cm^{-2}) is the anodic current density carried by X, D_x^{cd} (cm^2 s^{-1}) is the diffusion coefficient of X in cadmium, X_b^{cd} (mol cm^{-3}) is the concentration of X in bulk cadmium, δ_a^{cd} (cm) is the diffusion layer thickness in cadmium, D_x^{salt} (cm^2 s^{-1}) is the diffusion coefficient of X in the salt, X_b^{salt} (mol cm^{-3}) is the concentration of X in bulk salt and δ_a^{salt} (cm) is the diffusion layer thickness in the salt.

If the anode potential E_a is given, the concentration of element X on both sides of the anode surface (X_{as}^{cd}, X_{as}^{salt}) can be determined by solving eqns. (1), (2a) and (2b) under given bulk concentrations (X_b^{cd}, X_b^{salt}). Then the current density or each component can be calculated by eqns. (2a) and (2b). This calculation is iterated by testing different values of E_a until the sum of the calculated current components agrees with the total anodic current applied. The same model was used for the Cd cathode by reversing the direction of the current in eqns. (2a) and (2b). For the solid cathode, the activity of the element at the cathode surface in eqn. (1) is assumed to be one because of the metallic deposit and eqn. (2b) is used.

3. Model parameters

3.1. Diffusion layer thickness

The diffusion layer thickness is the most important parameter of the model. These thicknesses were determined on the basis of polarization data [4] measured for uranium in a 10 g scale ER using an Ag/0.1mol%AgCl reference electrode, as shown in Fig. 3(a). The diffusion layer thickness depends on the hydrodynamic condition near the electrode, so the following values should be considered as rough estimates and will need to be refined for the configuration and mixing condition of a specific ER. Moreover, the following estimates depend upon the values used for the diffusion coefficients of uranium in the salt, $D_x^{salt} = 5 \times 10^{-6}$ cm^2 s^{-1} [6], and in cadmium, $D_x^{cd} = 1.5 \times 10^{-5}$ cm^2 s^{-1} [7]. The use of larger diffusion coefficients will result in thicker diffusion layers.

The polarization data for the solid cathode depend on the uranium concentration in the salt. At a uranium concentration of 8.87 wt.% in the salt (in the following text the concentrations in the salt do not include the weight of chlorine in the chloride) there is no limiting current up to 1.5 A, as shown by the experimental data in Fig. 4. The *IR* drop is included in the potential change, so the slope of the curve represents the ohmic resistance between the cathode and reference electrode. Calculated results for various diffusion layer thicknesses (0.001, 0.002 and 0.010 cm) are also plotted in Fig. 4. The results for 0.010 cm are not appropriate because the increase in the current was limited to about 1 A,

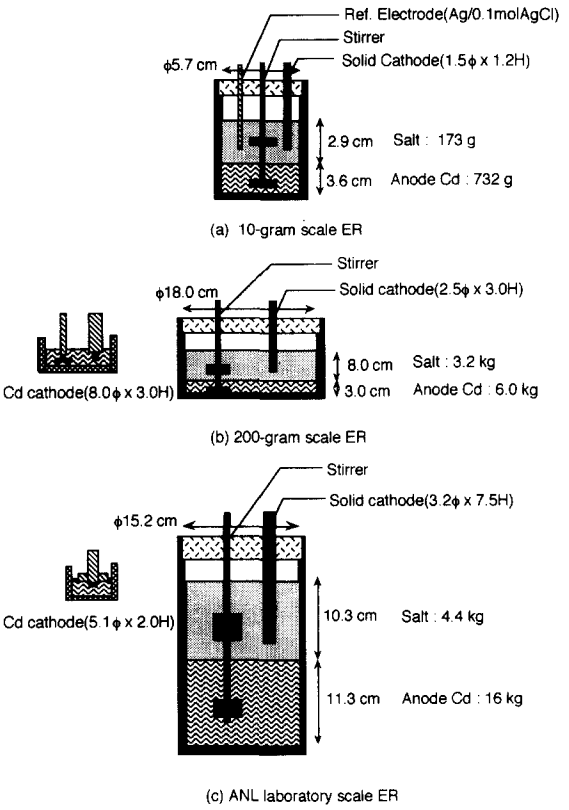

Fig. 3. Schematic diagrams of electrorefiners used to obtain the experimental data: (a) 10 g scale ER, (b) 200 g scale ER, (c) ANL laboratory scale ER.

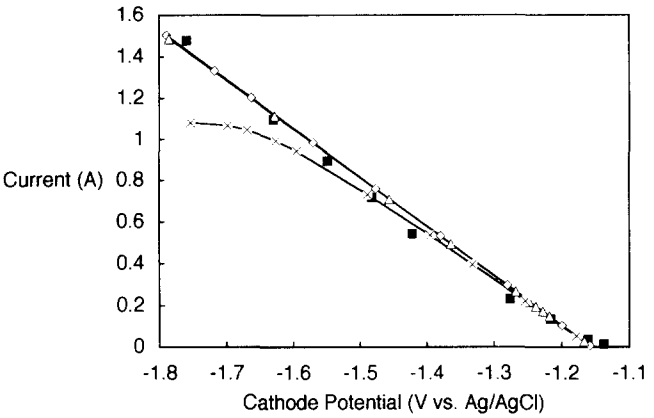

Fig. 4. Cathodic polarization curve for a uranium concentration of 8.87 wt.% in the salt measured in the 10 g scale ER (■) compared with calculated curves for diffusion layer thicknesses δ (cm) of 0.001 (◇), 0.002 (△) and 0.010 (×) on the salt side.

which is inconsistent with the experimental data. Thus the thickness should be less than 0.010 cm. At a concentration of 0.75 wt.% uranium in the salt the measured data started at −1.3 V and then polarized to −2.5 V, where lithium in the salt began to dominate the reduction current, as shown in Fig. 5. Calculations with the three layer thicknesses are also compared with the measured data in Fig. 5. This comparison suggests

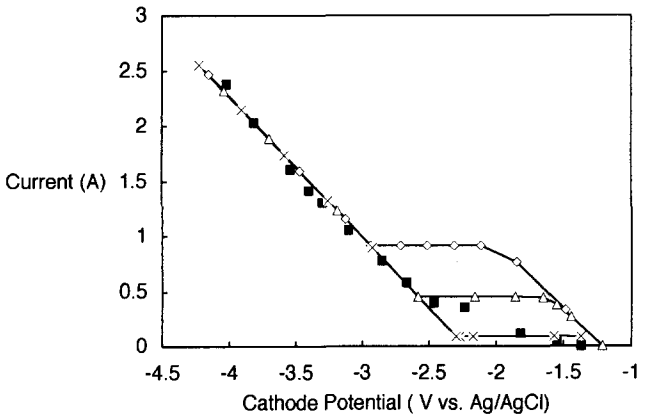

Fig. 5. Cathodic polarization curve for a uranium concentration of 0.75 wt.% in the salt measured in the 10 g scale ER (■) compared with calculated curves for diffusion layer thicknesses δ (cm) of 0.001 (◇), 0.002 (△) and 0.010 (×) on the salt side.

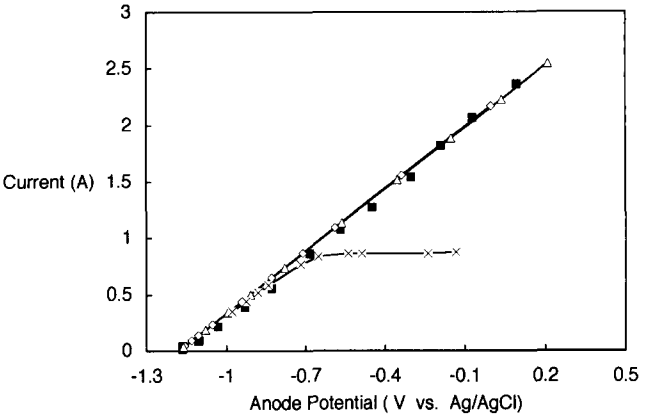

Fig. 6. Anodic polarization curve for a uranium concentration of 0.26 wt.% in cadmium measured in the 10 g scale ER (■) compared with calculated curves for diffusion layer thicknesses δ (cm) of 0.001 (◇), 0.002 (△) and 0.010 (×) on the cadmium side and 0.002 on the salt side.

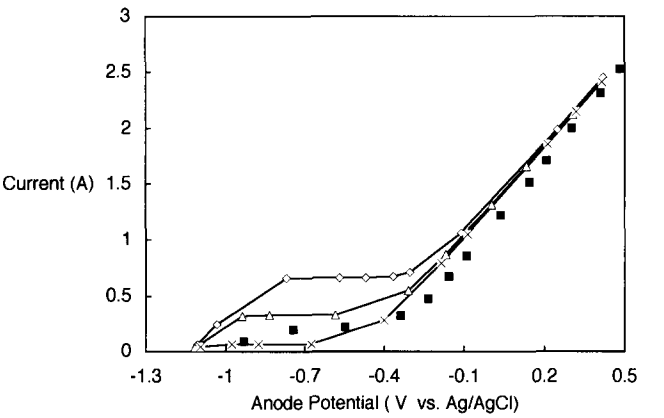

Fig. 7. Anodic polarization curve for a uranium concentration of 0.02 wt.% in cadmium measured in the 10 g scale ER (■) compared with calculated curves for diffusion layer thicknesses δ (cm) of 0.001 (◇), 0.002 (△) and 0.010 (×) on the cadmium side and 0.002 on the salt side.

that the diffusion thickness should be more than 0.001 cm, because the corresponding curve tends to overestimate the actual limiting current carried by the uranium in the salt. Therefore 0.002 cm was chosen for the diffusion layer thickness of the solid cathode.

For the Cd anode, two thicknesses have to be determined: one at the salt side, the other at the cadmium side of the salt–cadmium interface. The former thickness was approximated to be the same as that of the solid cathode (0.002 cm). This thickness is not so influential on the calculated result. On the other hand, the thickness at the cadmium side limits the mass transport across the interface owing to the lower solubility of uranium in cadmium compared with that of uranium chloride in the salt. To determine this thickness, two polarization measurements were compared with the calculated results for various thicknesses on the cadmium side. Following the same argument as used for the solid cathode, the thickness of 0.002 cm was chosen for the cadmium side of the Cd anode. The anodic polarization data (measured and calculated) for uranium concentrations of 0.26 and 0.02 wt.% in cadmium are shown in Figs. 6 and 7 respectively. The standard potential of uranium, −1.1 V *vs.* Ag/0.1mol%AgCl, was selected to reproduce the polarization data shown in Fig. 6.

At first, the thicknesses for the Cd anode were also applied to the Cd cathode because of their similarity. One experiment [5] was undertaken to investigate the deposition behaviour of the Cd cathode in the 200 g scale ER shown in Fig. 3(b). The calculated deposition history of uranium together with that for gadolinium and neodymium is shown in Fig. 8. The current efficiency (0.7) was used to adjust the amount of uranium deposited in the Cd cathode. This calculation underestimated the deposited amount of gadolinium. This discrepancy could be due to the use of the same layer thickness as the Cd anode, because the Cd cathode interface is more confined than that of the Cd anode. As a result, several calculations were made with layer thicknesses between 0.001 and 0.004 cm. It was found that the amount of gadolinium and neodymium was sensitive to the diffusion layer thickness for the salt side of the Cd cathode, as shown in Fig. 9. From this study, 0.003 cm was selected for the diffusion layer thickness of the Cd cathode.

3.2. Other parameters

The following activity coefficients in cadmium evaluated by Johnson and coworkers [8, 9] were used:

$$\gamma_U = 88.7, \qquad \gamma_{Pu} = 2.32 \times 10^{-4},$$

$$\gamma_{Gd} = \gamma_{Nd} = 1.13 \times 10^{-8}$$

where the activity coefficient of cerium [10] was substituted for those of neodymium and gadolinium.

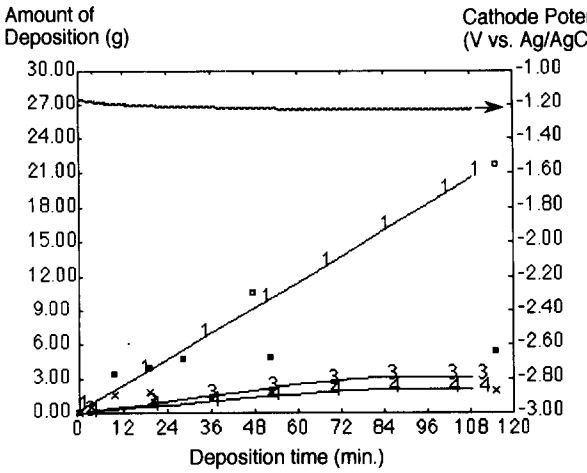

Fig. 8. Deposition history of the Cd cathode in the 200 g scale ER. The calculated depositions of uranium, gadolinium and neodymium are plotted as lines 1, 3 and 4 respectively compared with experimental values: □, U; ■, Gd; ×, Nd. The amounts of gadolinium and neodymium are multiplied by 50. The calculated cathode potential is plotted as a thick wavy line.

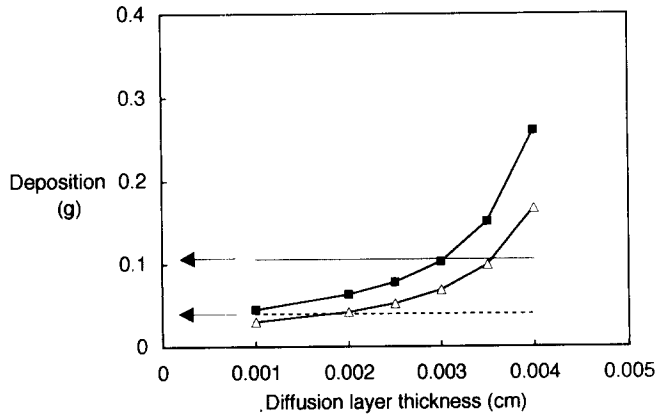

Fig. 9. Effect of diffusion layer thickness on calculated amounts of depositions of gadolinium (■) and neodymium (△) on the Cd cathode. The experimental values are shown by solid (Gd) and broken lines (Nd).

The activity coefficients of these elements in the salt were assumed to be the same, because little interaction is expected between these elements and the salt.

The standard potentials were determined by the following formulae relative to uranium:

$$E_o^{Pu} = E_o^U - \frac{RT}{3F} \ln\left(\frac{\gamma_U}{\gamma_{Pu}} SF_{Pu}\right) = -1.40 \text{ V}$$

$$E_o^{Gd} = E_o^U - \frac{RT}{3F} \ln\left(\frac{\gamma_U}{\gamma_{Gd}} SF_{Gd}\right) = -1.73 \text{ V}$$

$$E_o^{Nd} = E_o^U - \frac{RT}{3F} \ln\left(\frac{\gamma_U}{\gamma_{Nd}} SF_{Nd}\right) = -1.69 \text{ V}$$

where

$E_o^U = -1.10$ V *vs.* Ag/0.1mol%AgCl

which was determined by the polarization data as mentioned above.

In addition, the following separation factors

$$SF_x = \frac{X^{salt}}{X^{cd}} \Big/ \frac{U^{salt}}{U^{cd}}$$

for element X were determined from the equilibrium concentration (wt.%) between the salt and cadmium [11]:

$SF_{Pu} = 1.85$, $SF_{Gd} = 269$, $SF_{Nd} = 46.3$

The values for uranium previously mentioned were used for the diffusion coefficients in the salt and cadmium.

3.3. General validity of the model

The general validity of the model depends on the assumptions of eqns. (1), (2a) and (2b), which seem to hold in many electrorefining processes using molten salt as an electrolyte. However, the actual calculation requires the evaluation of the parameters in the given process. For the electrorefining process for an MFC which will operate at 773 K, the parameters evaluated in this section will be good enough for rough estimates. The accuracy of the prediction can be improved by refining the diffusion layer thicknesses using polarization curves measured for the specific ER. Calculations for other conditions (*e.g.* different temperatures and materials) require the evaluation of the thermodynamic parameters described in this section.

4. Verification

Three ANL experiments were used to verify the TRAIL code with regard to electrodeposition on the solid cathode, electrodeposition on the Cd cathode and dual-cathode operation. The calculation conditions for these runs are summarized in Table 1.

In the ANL laboratory scale ER shown in Fig. 3(c), series of runs (ANL Eng. Runs 27–30) were made [12] to investigate the behaviour of plutonium after successively removing uranium using the solid cathode. In the dual-cathode procedure mentioned previously, the solid cathode will be used only to remove uranium and concentrate plutonium in the salt. However, in this experiment the deposition with the solid cathode was continued further to study the extreme situation where plutonium starts to deposit on this cathode. Both the experiment and calculation indicated plutonium deposition in the final run, as shown in Fig. 10. In addition, a stepwise increase in the cell voltage predicted by the calculation was observed in the experiment, as shown in Fig. 11. The potentials of the electrodes were not measured, but the calculation predicted that this cell voltage increase was caused by the change in the cathode potential when plutonium started to deposit. The cal-

TABLE 1. Calculation conditions

	Eng. Run 27–30 (ANL lab. scale)	Eng. Run 20 (ANL lab. scale)	F16[a] (200 g scale)
Current (A)	1.0–2.0	2.0	3.6
Time (h)	56.7	26.1	8.3
Efficiency (%)	96	50	30
Deposit (g)	314.7 U 95% Pu 4.5% Nd < 0.01%	83.4 U 42% Pu 57% Nd 0.6%	20.2 U 18% Gd 72% Nd 10%
Initial concentration in salt (wt.%)	U 1.61 Pu 1.82 Nd 1.17	U 1.3 Pu 2.1 Nd 0.9	U 0.37 Gd 12.9 Nd 1.16
Initial concentration in Cd (wt.%)	U 1.01 Pu 0.59 Nd < 0.01	U 0.47 Pu 0.60 Nd 0.02	U 1.91 Gd 0.38 Nd 0.04
Final concentration in salt (wt.%)	U 0.08 Pu 3.1 Nd 1.08	U 1.17 Pu 2.7 Nd 0.8	U 0.22 Gd 12.1 Nd 1.05
Final concentration in Cd (wt.%)	U 0.01 Pu 0.27 Nd < 0.01	U 0.12 Pu 0.20	U 1.90 Gd 0.22 Nd 0.03

[a]Condition for Cd cathode in dual-cathode operation.

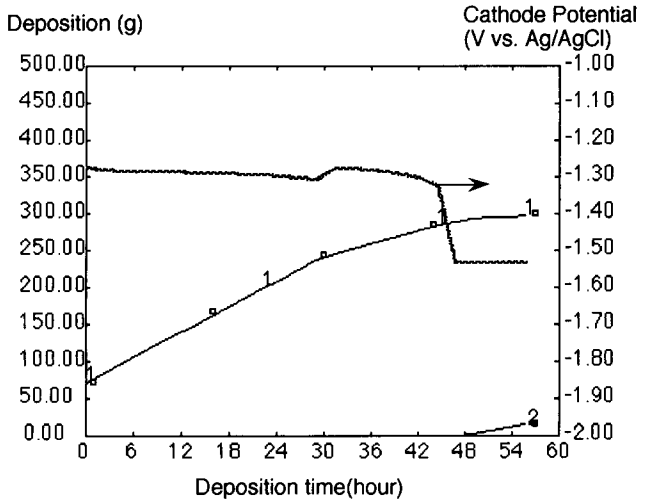

Fig. 10. Calculated deposition histories of uranium (line 1) and plutonium (line 2) on the solid cathode in ANL Eng. Runs 27–30 compared with corresponding experimental values (□, U; ■, Pu). The calculated cathode potential is plotted as a thick wavy line.

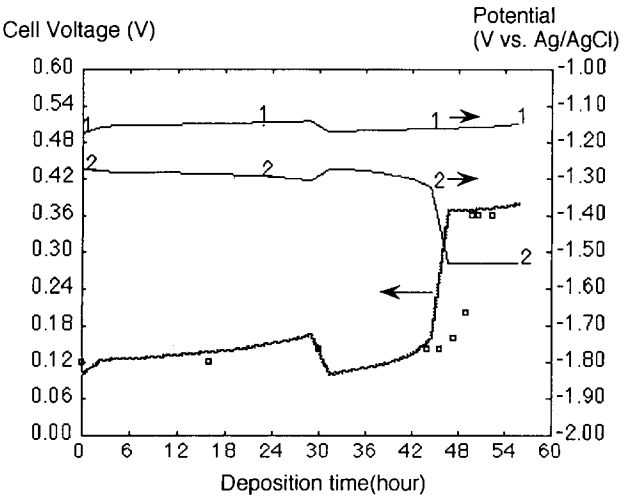

Fig. 11. Calculated cell voltage (thick wavy line) and anode (line 1) and cathode (line 2) potential changes during ANL Eng. Runs 27–30. The measured cell voltage is plotted as open squares.

culated concentration changes of uranium, plutonium and neodymium in the salt agree well with the experiment, as shown in Fig. 12. During this experiment the uranium removed from the salt was compensated by the increase in plutonium, while the concentration of neodymium did not change. The deposition of plutonium coincided with the depletion of uranium from the salt. The concentration changes in the Cd anode are plotted in Fig. 13. These results indicate that uranium was also depleted from the Cd anode and plutonium was gradually oxidized into the salt, while the zirconium concentration remained constant.

The codeposition of plutonium with uranium on the Cd cathode was studied in a run with the ANL laboratory scale ER (ANL Eng. Run 20) [13]. Because the activity coefficient of plutonium in cadmium is very low, as mentioned previously, plutonium can be codeposited

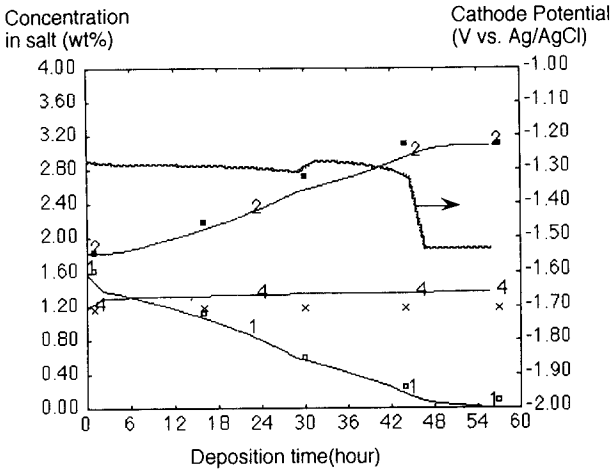

Fig. 12. Calculated concentration changes of uranium (line 1), plutonium (line 2) and neodymium (line 4) in the salt during ANL Eng. Runs 27–30 compared with corresponding experimental values (□, U; ■, Pu; ×, Nd). The calculated cathode potential is plotted as a thick wavy line.

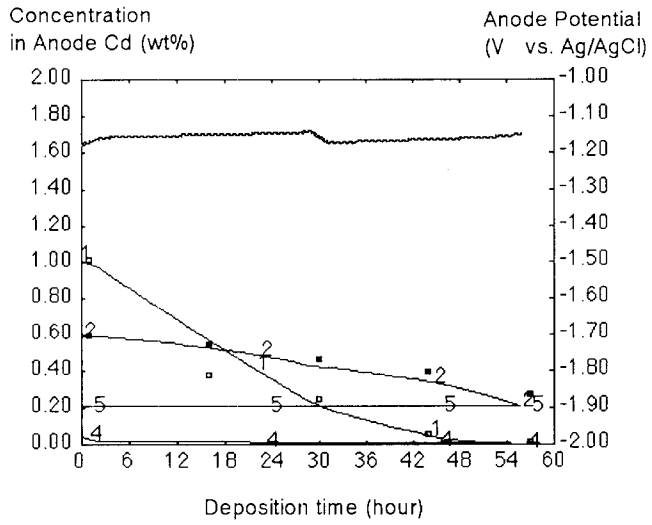

Fig. 13. Calculated concentration changes of uranium (line 1), plutonium (line 2), neodymium (line 4) and zirconium (line 5) in the Cd anode during ANL Eng. Runs 27–30 compared with corresponding experimental values (□, U; ■, Pu). The calculated cathode potential is plotted as a thick wavy line.

with uranium on the Cd cathode. The calculated deposition history of uranium, plutonium and neodymium is shown in Fig. 14 together with the corresponding experimental data (where the amount of neodymium is multiplied by 20). In this experiment the initial concentration of plutonium in the salt was too high relative to uranium, so the amount of plutonium was larger than that of uranium. Also, because of the high plutonium concentration, some neodymium was deposited, but the rate of deposition was not constant. The deposition of neodymium was predicted to stop after 6 h, when the Cd cathode was saturated with

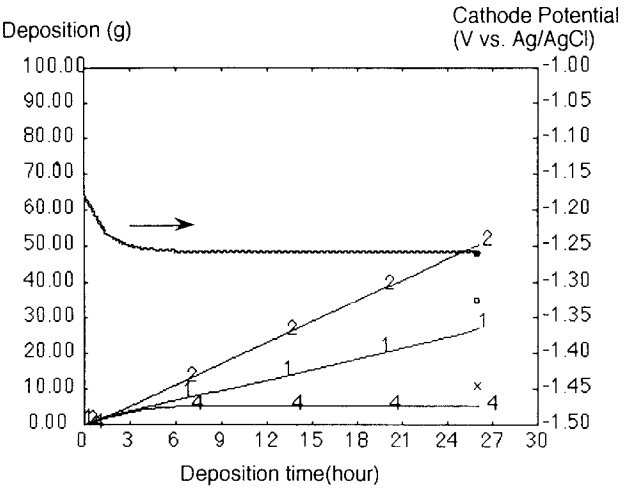

Fig. 14. Calculated deposition histories of uranium (line 1), plutonium (line 2) and neodymium (line 4) on the Cd cathode in ANL Eng. Run 20 compared with corresponding experimental values (□, U; ■, Pu; ×, Nd). The amount of neodymium is multiplied by 20. The calculated cathode potential is plotted as a thick wavy line.

plutonium and uranium. This can be explained by the following argument.

The cathode potential can be described by the Nernst equations

$$E_c = E_o^{Nd} + \frac{RT}{Z_{Nd}F} \ln\left(\frac{a_{Nd\ in\ salt}}{a_{Nd\ in\ Cd}}\right) \quad (3a)$$

$$= E_o^{U} + \frac{RT}{Z_{U}F} \ln\left(\frac{a_{U\ in\ salt}}{a_{U\ in\ Cd}}\right) \quad (3b)$$

$$= E_o^{Pu} + \frac{RT}{Z_{Pu}F} \ln\left(\frac{a_{Pu\ in\ salt}}{a_{Pu\ in\ Cd}}\right) \quad (3c)$$

where $a_{x\ in\ salt}$ and $a_{x\ in\ Cd}$ are the activities of the element X at the salt and cadmium sides of the Cd cathode interface respectively.

If the concentrations of all three elements at the salt side of the interface become constant, as shown in Fig. 15 after 6–9 h, and the cadmium in the cathode has already been saturated with uranium and plutonium, the cathode potential should be kept constant from eqns. (3b) and (3c). Then the activity of neodymium in the cadmium should be fixed from eqn. (3a). Thus the deposition of neodymium stops, while uranium and plutonium can keep depositing without changing the activity because they have already saturated the cadmium.

The other important observation is that the bulk concentrations of uranium and plutonium in the salt could differ significantly from the local concentrations at the interface, as shown in Fig. 15, which cannot be handled by an equilibrium model. The calculated bulk concentrations of uranium and plutonium in the Cd

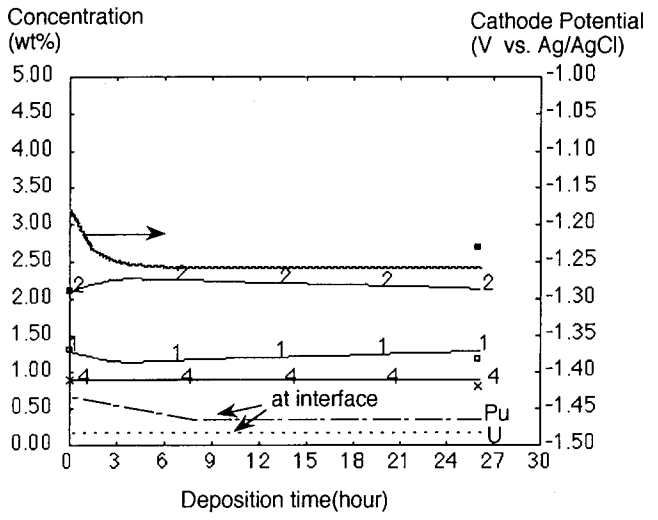

Fig. 15. Calculated concentration changes of uranium and plutonium at the salt side of the cathode interface (·····, – · – · – ·) as well as calculated bulk concentrations of uranium (line 1), plutonium (line 2) and neodymium (line 4) in the salt during ANL Eng. Run 20 compared with corresponding measured bulk concentrations (□, U; ■, Pu; ×, Nd). The calculated cathode potential is plotted as a thick wavy line.

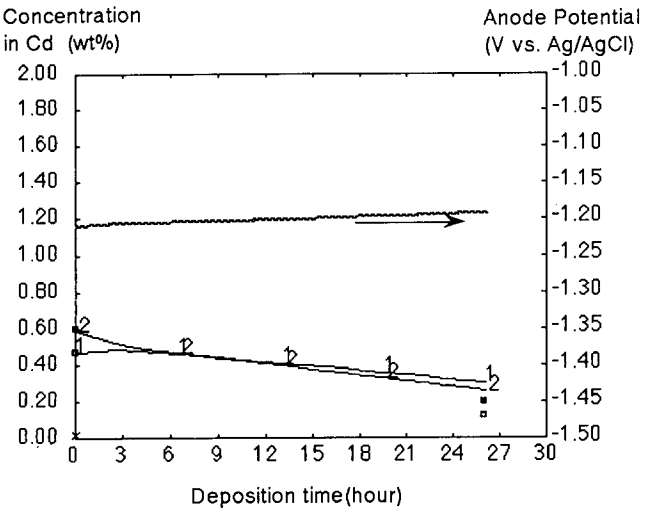

Fig. 16. Calculated concentration changes of uranium (line 1) and plutonium (line 2) in the Cd anode during ANL Eng. Run 20 compared with corresponding measured values (□, U; ■, Pu). The calculated anode potential is plotted as a thick wavy line.

anode also agree well with the experimental data, as shown in Fig. 16.

The dual-cathode operation was simulated in the 200 g scale ER using gadolinium as a substitute for plutonium [5]. The amount of deposition is plotted in Fig. 17, where the solid cathode was switched to the Cd cathode after 28 h. When the uranium was removed with the solid cathode, the concentration of uranium in the salt continuously decreased while that of gadolinium continuously increased, as shown in Fig. 18. Then gadolinium codeposited with uranium on the Cd cathode.

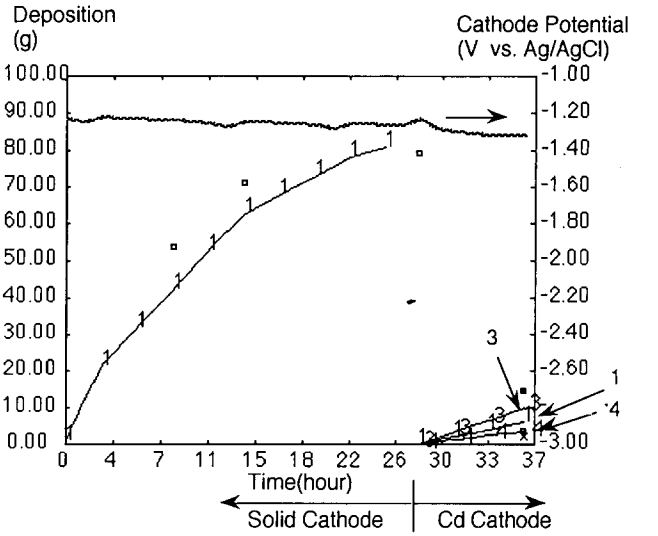

Fig. 17. Calculated deposition histories of uranium (line 1, gadolinium (line 3) and neodymium (line 4) during dual-cathode operation compared with the measured values (□, U; ■, Gd; ×, Nd). The calculated cathode potential is plotted as a thick wavy line.

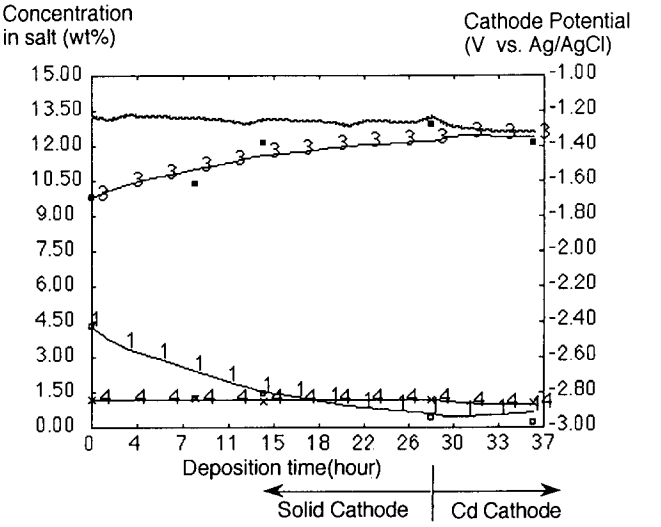

Fig. 18. Calculated concentration changes of uranium (line 1), gadolinium (line 3) and neodymium (line 4) during dual-cathode operation compared with measured values (□, U; ■, Gd; ×, Nd). The calculated cathode potential is plotted as a thick wavy line.

Since the electrochemical characteristics of gadolinium are much closer to those of neodymium than to those of plutonium, the deposition of neodymium was significant.

To compare these results with an equilibrium calculation, the TRAIL code was used with artificially small diffusion thicknesses on the electrodes (one-tenth of the above optimized thicknesses) so that the local concentrations approached the equilibrium values. The depositions predicted by these two calculations are plotted in Fig. 19 together with the experimental values. This comparison indicates the significant deviation of

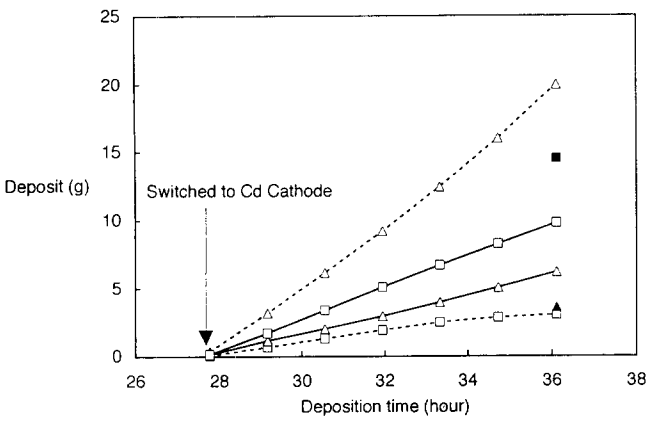

Fig. 19. Comparison of deposition of uranium (△) and gadolinium (□) on the Cd cathode by TRAIL (solid lines) and equilibrium analysis (broken lines). The filled triangle and square are experimental values for U and Gd respectively.

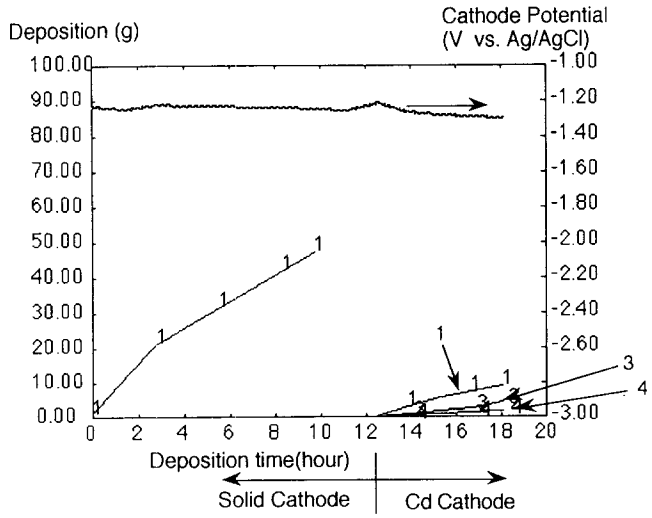

Fig. 20. Calculated deposition histories of uranium (line 1), gadolinium (line 3) and neodymium (line 4) during improved dual-cathode operation. The calculated cathode potential is plotted as a thick wavy line.

the system from equilibrium, because the result with thinner layer thicknesses (equilibrium calculation) predicted the predominant deposition of uranium, while gadolinium deposited more in the experiment. Thus the calculation with optimized thicknesses was much closer to the experiment.

Another calculation was made to investigate the possibility of controlling the composition of the deposit on the Cd cathode. To decrease the ratio of gadolinium in the deposit, the solid cathode was switched to the Cd cathode after 12 h. The amount of gadolinium on the Cd cathode became less than that of uranium, as shown in Fig. 20. Thus this calculation demonstrated the possibility of controlling the composition of the deposit by changing the timing of the switch to the Cd cathode.

5. Summary

A simulation code (TRAIL) for the molten salt electrorefining of spent metallic nuclear fuel has been developed. This code employs diffusion layer theory in the vicinity of the electrodes. Model parameters such as the diffusion layer thickness were determined from polarization data measured with uranium at different concentrations in the molten salt electrolyte and liquid cadmium anode. The optimized diffusion layer thickness was determined to be 0.002 cm for the solid cathode and Cd anode. For the Cd cathode, 0.003 cm was chosen after studying the composition of the deposit on the Cd cathode.

Then TRAIL calculations were made to verify the code with experimental data for various operational modes. Good agreement with the data was obtained. This analysis also predicted the deviation of local concentration in the vicinity of the electrodes from the bulk concentration in the salt.

In the dual-cathode operation, when the uranium concentration in the salt is very low, this code can provide better results than calculations assuming equilibrium, which cannot reproduce the experimental data. Calculations using the TRAIL code also revealed that the composition of the deposit on the Cd cathode can be controlled by adjusting the time of switching of the cathode in the dual-cathode operation.

Acknowledgments

The authors owe the idea of applying the diffusion layer theory to Professor Y. Ito of Kyoto University. The authors are grateful to colleagues of the Chemical Technology Division of ANL for providing the experimental data for code verification under the contract of the Joint Program on IFR Technology between CRIEPI and US DOE. In particular, Dr. J. E. Battles, Dr. J. P. Ackerman and Dr. J. Harmon of ANL reviewed the manuscript and gave the authors valuable advice. Thanks are also given to Dr. K. Kikuta (currently working at Hachinohe Smelting Co. Ltd.) and Dr. Y. Sumida of the Nuclear Engineering Laboratory of Toshiba Corp. for providing details of the Japanese experimental data.

References

1 Y. I. Chang, The Integral Fast Reactor, *Nucl. Technol.*, *88* (1989) 129.

2 J. E. Battles, W. E. Miller and E. C. Gay, Pyrometallurgical processing of Integral Fast Reactor metal fuels, *Int. Conf. on Nucl. Fuel Processing and Waste Management, British Nad. Forum, Sendai, Japan, 1991*, p. 342.

3 J. P. Ackerman, Chemical basis for pyrochemical reprocessing of nuclear fuel, *Ind. Eng. Chem. Res., 30* (1) (1991) 141–145.
4 M. Tokiwai, T. Koyama, *et al.,* Molten salt electrorefining of metallic fuel. I. Electrotransportation of uranium, *AECS Meeting, Phoenix, AZ, 1991,* p. 279.
5 T. Koyama, T. Kobayashi, *et al.,* Molten salt electrorefining of metallic fuel. II. Electrorefining of U and Nd, *AECS Meeting, Phoenix, AZ, 1991,* p. 280.
6 D. S. Poa, Z. Tomczuk and R. K. Stunenberg, Voltametry of uranium and plutonium in molten LiCl–NaCl–$CaCl_2$–$BaCl_2$. I. Reduction of U(III) to uranium metal, *J. Electrochem. Soc., 135* (1988) 1161.
7 J. C. Hesson, H. E. Hootman and L. Burris Jr., *J. Electrochem. Technol., 3* (1965) 240.
8 I. Johnson, M. G. Chasanov and R. M. Yonco, Pu–Cd system: thermodynamics and partial phase diagram, *Trans. Metall. Soc. AIME, 233* (1965) 1408.
9 I. Johnson and H. M. Feder, Thermodynamics of the uranium–cadmium system, *Trans. Metall. Soc. AIME, 224* (1962) 468.
10 I. Johnson and R. M. Yonko, Thermodynamics of cadmium- and zinc-rich alloys in the Cd–La, Cd–Ce, Cd–Pr, Zn–Ce and Zn–Pr systems, *Metall. Trans, 1* (1970) 905.
11 J. P. Ackerman, Argonne National Laboratory, personal communication, 1991.
12 Z. Tomczuk, J. P. Ackerman, R. D. Wolson and W. E. Miller, Uranium transport to solid electrodes in pyrochemical reprocessing of nuclear fuel, *J. Electrochem. Soc., 139* (12) (1992) 3523.
13 Z. Tomczuk, Argonne National Laboratory, personal communication, 1991.